

THREE-DIMENSIONAL FREE WAKE CALCULATION OF WIND TURBINE WAKES

A.ZERVOS¹, S.HUBERSON² and A.HEMON³

¹Laboratory of Aerodynamics, National Technical University of Athens,
42, 28th Octovriou Str, 10682 Athens, Greece

²Laboratoire d'Informatique pour la Mécanique et les Sciences de l'Ingénieur
(L.I.M.S.I.), B.P.30-91406 Orsay Cedex, France

³Sté GENIMAR, 21-23 rue Lalande, 75014 Paris, France

SUMMARY

A numerical method has been developed for the computation of wake structure and development of horizontal axis wind turbines. The method uses the vortex particle concept which already has been used in order to compute three-dimensional unsteady inviscid flows around wings and helicopter rotors. It is a grid-free Lagrangian free vortex method in which vorticity is discretized into a set of vortex carrying particles. The time evolution of each particle is being computed independently at each time step. The blades are represented as lifting surfaces and the exact geometry (including the nacelle) is taken into account. The governing equations are the vorticity transport equations and the Biot-Savart law expressed in Lagrangian coordinates. The method was applied for the calculation of the wake characteristics of a HAWT whose geometry was chosen in correspondence to existing experimental results so that comparisons could be possible. The results include velocity profiles and vortex particles positions and velocities in the wake of the WT. In order to simulate the performance of the WT in a wind park arrangement the interaction between two turbines was calculated.

INTRODUCTION

A great effort has been undertaken recently on an international level in order to produce more accurate wind farm power prediction models (ref.1). From the experience of the last years it has become clear that the wake interaction calculations play an important role in the accuracy of these models and become determinant if the loading of the wind farm's turbines has to be predicted.

The wind farm models can be classified into three categories:

- a) The kinematic semi-empirical models based on global momentum conservation assumptions and on an analogy of the wake velocity profiles with the profiles in free jets. The first model was developed by Lissaman (ref.2). Vermeulen (ref.3) obtained an ameliorated version by combining a similar theoretical approach with experimental data.
- b) The eddy-viscosity model developed by Ainslie (ref.4). In this model the axisymmetric boundary layer approximation of the Navier-Stokes equations is solved in order to simulate the wake flow and the eddy-viscosity is modelled by

an analytical expression.

c) The $k-\epsilon$ type model developed by Crespo et al (ref.5 and 6) where the wake is also simulated by solving the boundary layer approximation of the Navier-Stokes equations using, though, a more sophisticated turbulence modelling ($k-\epsilon$).

A detailed survey of the above models was presented recently by Luken(ref.7).

A common characteristic of all the models is that they are time independent and as a consequence they can not predict certain effects which are inherent to the unsteadiness of the flowfield. As an example we can mention the calculation of the load variations of a wind turbine immersed in the wake of other wind turbines.

Even the more advanced of the existing models, although they describe adequately the turbulence of the wake flow, they require empirical values of certain parameters. The particular characteristics of the wind turbine (form of blades, pitching etc) are not taken into account. They can, though, become important when the prediction of load fluctuations on the rotor blades are needed.

The method proposed in this work is of a completely different type and tries to cover these drawbacks of the other methods. On the other hand, it can not give the same amount of information on certain parameters (such as turbulence) and as a consequence it can be considered as complementary to the other methods.

The basic aim of the present work is to produce a detailed description of a wind turbine wake (near and developed) as well as of the flowfield behind a WT immersed in the wake of another WT. The three dimensional unsteady free wake vortex particle method with its Lagrangian grid-free description of the flow field is used. The method does not use any empirical values. The required inputs are the exact geometry of the wind turbine (incorporating nacelle, tower etc) and the form of the incident wind velocity profile.

The basic drawback of the method for a complete wind farm calculation is the prohibitive computer time when several WT have to be calculated simultaneously.

METHOD OF SOLUTION

The three-dimensional unsteady vortex particle method has been introduced first by Rhebach (ref.8) in order to compute inviscid flows around thin wings. It was extended to flows around bodies in arbitrary motions by Huberson(ref.9) and applied to helicopter rotor problems by Cantaloube and Huberson (ref.10). The method was adopted by Huberson and Zervos (ref.11) in order to treat the problem of Vertical Axis Wind Turbines.

The governing equations are the vorticity transport equations and the Biot-Savart law expressed in Lagrangian coordinates:

$$\frac{d\vec{\omega}}{dt} = (\vec{\omega} \cdot \vec{\nabla}) \vec{U} \quad (1)$$

$$\frac{d\vec{x}}{dt} = \vec{U} \quad (2)$$

$$\vec{U} = \frac{1}{4\pi} \iiint \frac{\vec{\omega}(\vec{x}') \wedge (\vec{x} - \vec{x}')}{|\vec{x} - \vec{x}'|^3} d\vec{x}' \quad (3)$$

where \vec{x} is the Lagrangian variable, \vec{U} the velocity field and $\vec{\omega}$ the rotational of \vec{U} . A potential φ is constructed in order to satisfy the boundary conditions on solid walls through a doublet distribution which is computed as a solution of an integral equation.

The wake vorticity distribution is discretized into a set of vortex carrying particles, whose intensity and position must satisfy the relations:

$$\vec{\Omega}_i = \iiint_{P_i} \vec{\omega} d\vec{x} \quad (4)$$

$$\vec{x}_i \wedge \vec{\Omega}_i = \iiint_{P_i} \vec{x} \wedge \vec{\omega} d\vec{x} \quad (5)$$

where P_i is the volume of the particle. Using equation (3) we can compute analytically an integral representation of equation's (1) right hand side. If, then, we introduce in equations (1) and (2) the discrete representation defined by (4) and (5) we get the following set of equations:

$$\frac{d\vec{x}_i}{dt} = \frac{1}{4\pi} \sum_{j \neq i} \frac{\vec{\Omega}_j \wedge (\vec{x}_i - \vec{x}_j)}{|\vec{x}_i - \vec{x}_j|^3} + \nabla \varphi|_{\vec{x}_i} \quad (6)$$

$$\begin{aligned} \frac{d\vec{\Omega}_i}{dt} = & \frac{3}{8\pi} \sum_{j \neq i} \frac{1}{|\vec{x}_i - \vec{x}_j|^5} [((\vec{x}_j - \vec{x}_i) \cdot \vec{\Omega}_i)(\vec{x}_i - \vec{x}_j) \wedge \vec{\Omega}_j + \\ & + ((\vec{x}_j - \vec{x}_i) \wedge \vec{\Omega}_j) \cdot \vec{\Omega}_i)(\vec{x}_j - \vec{x}_i)] + (\vec{\Omega}_i \cdot \vec{\nabla}) \nabla \varphi|_{\vec{x}_i} \end{aligned} \quad (7)$$

In the discretization process the rotor surface is represented by N panels. On each panel a constant doublet distribution μ is assumed. The potential φ is expressed as an integral function of the doublet distribution μ and μ is found through the solution of the following integral equations expressing the zero-normal velocity condition (slip condition) on the solid surfaces S :

$$\iint_S \mu \cdot \vec{n} \cdot \vec{\nabla} \left(\frac{\vec{x}' - \vec{x}}{|\vec{x}' - \vec{x}|^3} \cdot \vec{n}' \right) d\vec{x}' = 4\pi (\vec{U}_\infty + \vec{U}_i) \cdot \vec{n} \quad (8)$$

where U_i is the velocity induced by the flow vorticity and U_∞ is the infinite boundary condition. This equation is satisfied at the center of each panel giving a system of N linear algebraic equations with unknowns the N values of

μ on the panels.

The surface distribution μ and the vorticity w are related by a modelisation of the trailing edge shedding through the application of the unsteady Kutta condition. This phenomenon is supposed to occur along given lines where vorticity is emitted.

The resulting vorticity of the particles is fixed using Bernoulli equation written on each side of these lines denoted + and -

$$\frac{d\Gamma}{dt} = \frac{|\vec{U}^+ + \vec{U}^-|}{2} |\vec{U}^+ - \vec{U}^-| \quad (9)$$

This model is an extension of two-dimensional models used by Luu (ref.12) or Basu and Hancock (ref.13). The particle emitted along a segment with length Δl , during a time interval Δt will be defined by:

$$\vec{\Omega}_i = \left(\Delta t \frac{|\vec{U}^+ + \vec{U}^-|}{2} \Delta l \right) |\vec{U}^+ - \vec{U}^-| \quad (10)$$

$$\vec{x}_i = \vec{x}_e + \frac{(\vec{U}^+ + \vec{U}^-)}{4} \Delta t \quad (11)$$

where \vec{x}_e is the center of the segment.

When the body is moving with a velocity \vec{U}_e , the absolute velocity \vec{U}_a , and the absolute vorticity $\vec{\Omega}_a$ verify the following relations:

$$\vec{U}_a = \vec{U}_r + \vec{U}_e \quad (12)$$

$$\vec{\Omega}_a = \vec{\Omega}_r + \vec{\Omega}_e \quad (13)$$

where \vec{U}_r and $\vec{\Omega}_r$ are the relative velocity and the relative vorticity respectively.

The extension of the algorithm to flows incorporating moving boundaries is readily obtained expressing equation (1) for absolute vorticity in the relative frame

$$\frac{d\vec{\Omega}_a}{dt} = (\vec{\Omega}_a \cdot \vec{\nabla}) \vec{U}_r - \vec{\Omega}_e \wedge \vec{\Omega}_a \quad (14)$$

The boundary conditions are modified to account for the frame velocity and we get

$$\frac{\partial \varphi}{\partial n} = (\vec{U}_\infty + \vec{U}_r + \vec{U}_e) \cdot \vec{n} \quad (15)$$

$$\frac{d\Gamma}{dt} = \left| \frac{\vec{U}^+ + \vec{U}^-}{2} + \vec{U}_e \right| |\vec{U}^+ - \vec{U}^-| \quad (16)$$

The flow being unsteady, a discretization into elementary intervals of time Δt is introduced and the field is resolved at each of these intervals. Between instants $t-\Delta t$ and t a set of vortex particles is created, leaving the trailing edge, and the position and intensity of all previously generated vortex particles is computed.

RESULTS

The method was applied for the calculation of the wake characteristics of a horizontal axis wind turbine. The geometry of the turbine (Fig.1) was chosen in correspondence to available to the authors experimental wind-tunnel results (ref.14) so that comparisons could be possible. The nacelle was also included in the simulation. Each rotor blade was represented by 25 panels and 105 panels were used to describe the nacelle.

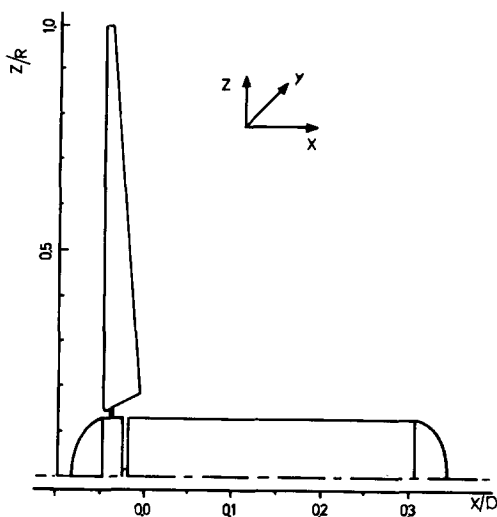


Fig.1 Schematic of the wind turbine

Emphasis was given in the calculation of the structure of the near wake, where little information is available. Figure 2 presents the positions of the vortex particles and their velocity vectors in three dimensions at a given instant for a distance of one diameter downstream of the rotor. Three sections are presented (each perpendicular to one of the axis) so that a complete qualitative view of the structure of the near wake can be seen. Important variations of the velocity vector direction can be clearly seen from the x-z and x-y projections, especially near the center region. From the y-z projection a tendency of the near wake to rotate is also presented. The calculations are

made at a tip speed ratio $\lambda=4$, which corresponds to the maximum efficiency of the turbine.

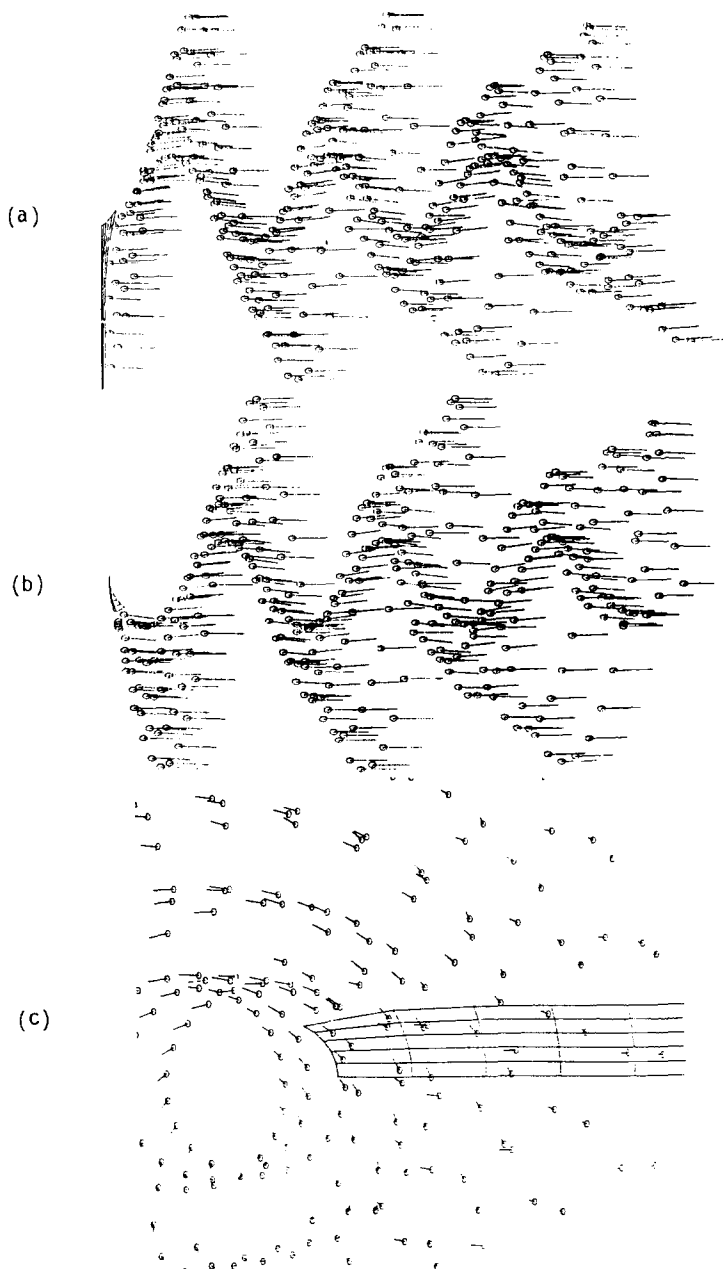


Fig.2. Positions of vortex particles and their velocity vectors at a given instant for $\lambda=4$. (a) x-z projection. (b) x-y projection. (c) y-z projection.

In Figure 3 the velocity deficit profiles at different sections downstream of the rotor are presented for the same tip speed ratio together with the corresponding experimental results (ref.14). The augmentation of the velocity deficit with downstream distance in the very near wake is evident. There is an agreement between the numerical and the experimental results as to the maximum velocity deficit for each section, but the radial distance at which this maximum occurs is not the same. This difference as well as the considerable deviation of the results as we approach the tip region are to a large amount due to the wind tunnel wall effects for the experimental results (the blockage for the experiment was of the order of 30%).

The wake development for a larger distance (four diameters) downstream of the wind turbine is presented in a similar manner in figures 4 and 5 for a different tip speed ratio ($\lambda=6$). A smoothing of the velocity vector direction variations as we move downstream of the rotor can be noticed from the x-y and x-z projections, while the rotational tendency of the wake is decreasing (smaller velocity vectors in the y-z projection). In figure 5 the velocity deficit profiles are presented at different sections up to 3.5 diameters downstream of the rotor. The velocity deficit starts decreasing after a distance of half diameter downstream of the rotor.

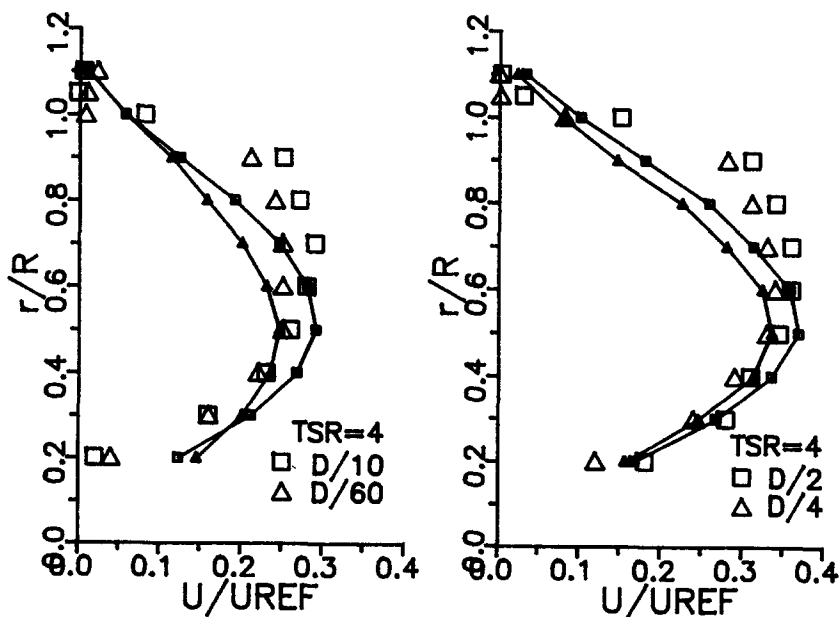
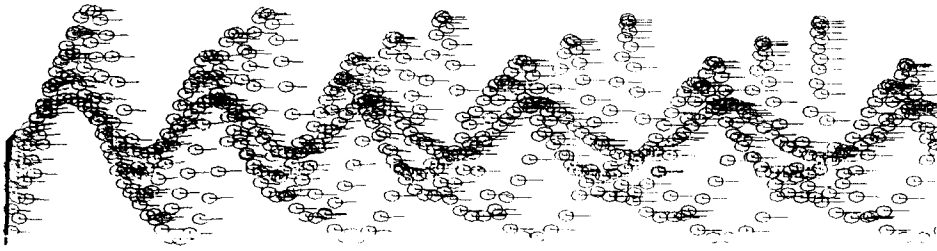
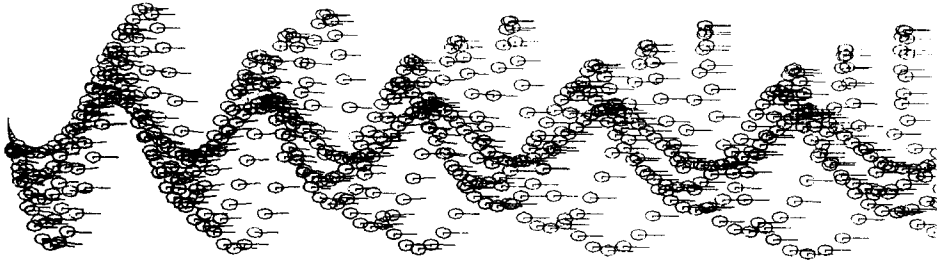


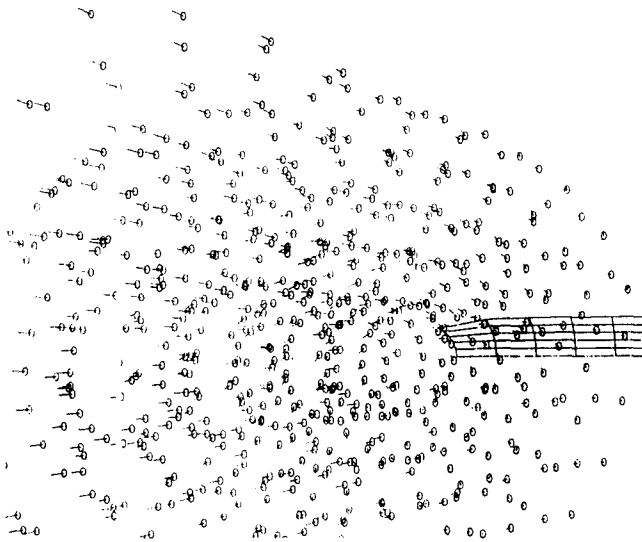
Fig.3. Comparisons of numerical and experimental results for velocity deficit profiles at different sections downstream of the rotor ($\lambda=4$).



(a) x-z projection



(b) x-y projection



(c) y-z projection

Fig. 4. Positions of vortex particles and their velocity vectors at a given instant for $\lambda=6$.

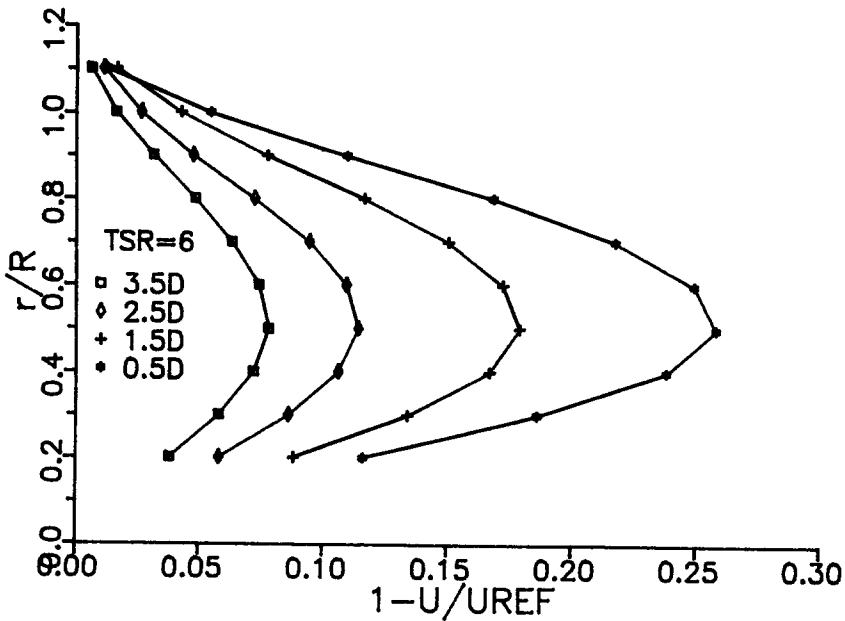
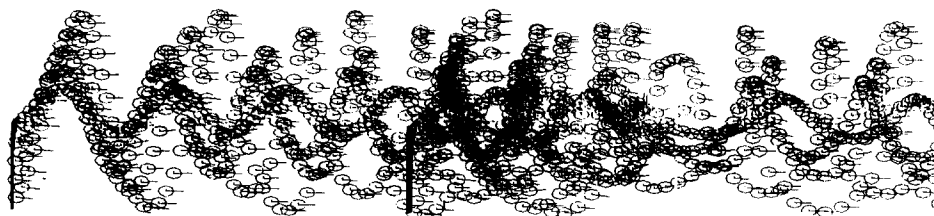


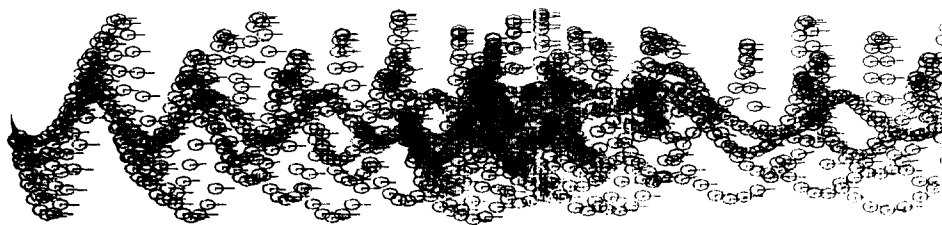
Fig.5. Velocity deficit profiles at different sections downstream of the rotor for $\lambda=6$.

In order to simulate the performance of a WT in a wind park arrangement, the interaction between two turbines is calculated. The positions and velocity vectors of the vortex particles presented in Fig. 6 show a large concentration of vortices behind the second turbine creating a strong unsteadiness of the flow field in that region. From the y - z projection we can see large radial velocity components in that region as a result of the mixing of the two wakes. In Fig. 7 velocity deficit profiles behind the second turbine are presented for $\lambda=4$. There is a considerable augmentation of the deficit as compared to the equivalent values behind the first turbine. As we move downstream the form of the profiles changes, the deficit augmenting from the center to the tip and decreasing from the center to the root.

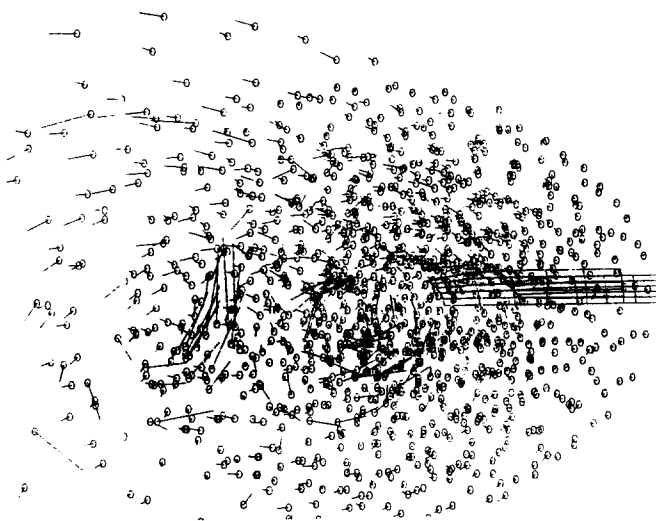
The ability of the model to incorporate non uniform wind velocities is shown through a calculation using a wind velocity profile simulating atmospheric boundary layer. The velocity field behind the turbine is presented in Fig. 8 by the iso-velocity curves in y - z projection.



(a) x-z projection



(b) x-y projection



(c) y-z projection

Fig. 6. Positions of vortex particles and their velocity vectors for two wind turbines at a distance of two diameters between them ($\lambda=4$).

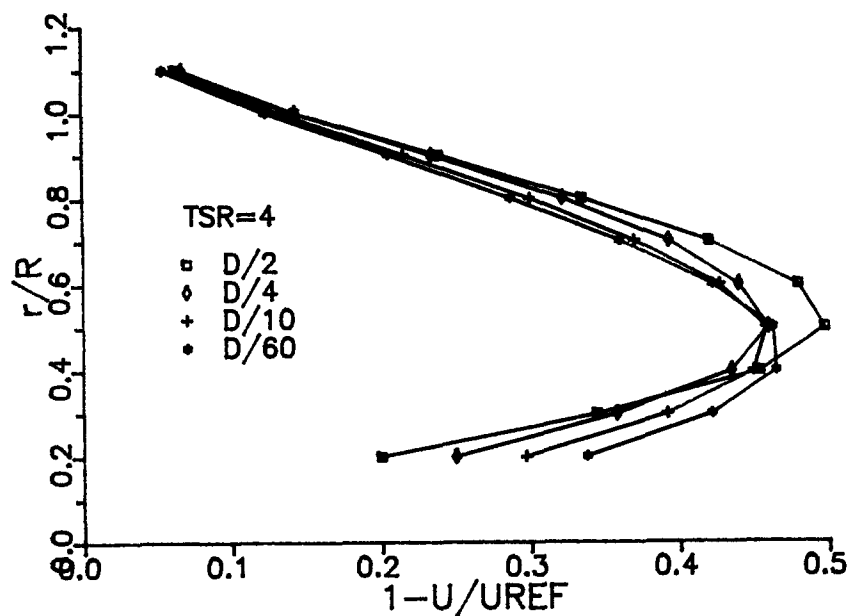


Fig.7. Velocity deficit profiles downstream of the WT immersed in the wake of another WT for $\lambda=4$.

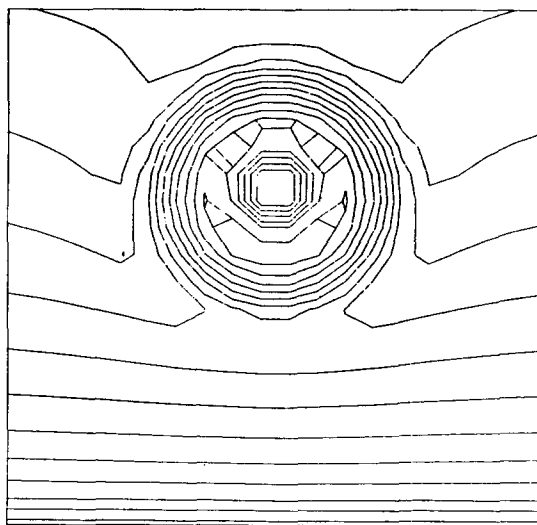


Fig.8. Iso-velocity curves in y-z protection at one diameter downstream of the rotor, for a wind velocity profile incorporating the atmospheric boundary layer.

CONCLUSIONS

A new method has been presented for the calculation of the wake of horizontal axis wind turbines. The method can describe the near as well as the developed wake and it can treat the problem of a wind turbine immersed in the wake of another turbine. On the other hand, the computer time needed for the calculation of a complete wind farm arrangement is prohibitive. The knowledge though, of the detailed structure of the wakes and of their interaction can produce better simplified models needed for the design of wind farms.

REFERENCES

- 1 L.van der Snoek, Development and validation of wind farm models, Int. Conf. on Wind farms, Leewarden, 1987
- 2 P.B.S. Lissaman, Energy effectiveness of arbitrary arrays of wind turbines, AIAA paper 79-0114, 1979.
- 3 P.E.J. Vermeulen, An experimental analysis of wind turbine wakes, 3rd Int. Symp. on Wind Energy Systems, Copenhagen, 1980.
- 4 J.F. Ainslie, Development of an eddy-viscosity model for wind turbine wakes, 7th BWEA Conference, 1985.
- 5 A Crespo, F.Manuel, D.Moreno, E.Fraga, J.Hernandez, Numerical analysis of wind turbine wakes, Workshop on wind energy applications, Delphi, 1985.
- 6 A Crespo, J. Hernandez, A numerical model of wind turbine wakes and wind farms, EWE Conference, Rome, 1986.
- 7 E.Luken, P.E.J. Vermeulen, Development of advanced mathematical models for the calculation of wind-turbine wake-interaction, EWE Conference, Rome, 1986.
- 8 C.Rehbach, Numerical calculation of three-dimensional unsteady flows with vortex sheet, AIAA, paper 78-111, 1978.
- 9 S.Huberson, Calcul d'écoulements tridimensionnels instationnaires incompressibles par une méthode particulaire, J.de Mécanique Théorique et Appliquée, vol. 3, (1984), 805-819.
- 10 B.Cantaloube and S.Huberson, Calcul d'écoulements de fluide incompressible non-visqueux autour de voilures tournantes par une méthode particulaire, La Recherch Aéronautique, 1984, 6, 403-415.
- 11 S. Huberson and A.Zervos, A three dimensional vortex particle model for the Darrieus rotor, submitted for publication.
- 12 T.S.Luu and J.Corniglion, Ecoulement instationnaire non linéaire autour d'un profil ou d'une grille d'aube avec émission de tourbillons libre, ATMA, 1972, 1-13.
- 13 B.C.Basu and G.J.Hancock, The unsteady motion of a two-dimensional aerofoil in incompressible inviscid flow, J.Fluid Mech., vol. 87, (1978), 159-178.
- 14 A.Papaconstantinou and G.Bergeles, Hot wire measurements of the flowfield in the vicinity of a HAWT rotor, submitted for publication.